American Mineralogist, Volume 81, pages 1176–1185, 1996

Optimizing the electron microprobe analysis of hydrous alkali aluminosilicate glasses

GEORGE B. MORGAN VI AND DAVID LONDON

Electron Microprobe Laboratory, University of Oklahoma, 100 East Boyd Street, 810 Sarkeys Energy Center, Norman, Oklahoma 73019-0628, U.S.A.

ABSTRACT

The time-dependent loss of Na$K\alpha$ X-ray intensity during electron-beam irradiation of hydrous alkali aluminosilicate glasses is apparently more significant during the initial few seconds of beam exposure than it is for anhydrous glasses, and it is pronounced for incident beam currents >2–5 nA (using 15–20 μm beam diameters). Exponential fits of Na$K\alpha$ intensity vs. time show a progressive decrease in the apparent zero-time intercepts for incident beams from 2 to 20 nA, and thus methods for correcting Na concentrations solely on the basis of curve fitting and extrapolation to zero-time values may underestimate Na contents by almost 10% (relative) for higher beam currents. Similar exponential fits to the intensity-time data for Al$K\alpha$ and Si$K\alpha$ show that "grow-in" is greater for Al than for Si. For incident currents $\geq$5 nA, the magnitudes of all intensity changes also increase with total H_2O content of glass. On the basis of these observations, the optimal conditions for analysis of hydrous alkali aluminosilicate glasses include a 2 nA beam with 20 μm diameter and counting times of 20–40 s for the analysis of alkali aluminosilicate components, with Na and Al analyzed first (simultaneously, if possible). These methods minimize Na loss and grow-in for Al and Si to the point that little or no correction is needed, provide good statistical accuracy, and work with a wide variety of standard materials (i.e., glass standards with compositions and H_2O contents comparable to the unknowns are not needed). For complete analysis of more complex multicomponent systems, two beam conditions are recommended: an initial 2 nA, 20 μm diameter beam for analysis of alkali aluminosilicate components, followed by a 20 nA, 20 μm diameter beam for analysis of all other components. With the use of these methods, the H_2O contents of hydrous glasses (H_2O as the only unknown) can be determined by difference with uncertainties mostly <5% (relative to FTIR values) for glasses containing up to 10 wt% H_2O. At beam currents >5 nA, corrections for Na loss ignoring Al (and Si) grow-in underestimate H_2O contents by about 10–50% of concentration.

INTRODUCTION

The loss of Na$K\alpha$ X-ray intensity during the electron microprobe analysis (EMPA) of silicate glasses has been known for decades (e.g., Varshneya et al. 1966; Kushiro 1972; Watkins et al. 1978) and has been the subject of both descriptive and mechanistic study (e.g., Lineweaver 1962; Borom and Hanneman 1967; Vassamillet and Caldwell 1969; Goodhew and Gulley 1974; Goodhew 1975; Spray and Rae 1995). Such studies showed decreases in Na count rate with increasing incident beam current, reduced beam diameter, and reduced accelerating potential. The loss of Na counts is attributed to migration of Na from the beam excitation volume. For comparatively immobile components, such as Si and Al, count rates increase with prolonged beam exposure, a phenomenon termed "grow-in." The grow-in of intensities for immobile components during glass analysis undoubtedly involves increases in their relative concentrations because of the migration of mobile components (alkalis and H_2O) from the excitation volume. The grow-in of Al and Si intensities accompanying Na migration is also likely to involve decreased absorption of their X-rays by Na. Empirical methods of correcting for (and cryogenic methods for avoiding) Na loss during microprobe analysis have been developed from studies on anhydrous glasses (e.g., Nielsen and Sigurdsson 1981), but to date little attention has been given to the analysis of hydrous glasses. In geologic studies, these include volcanic glasses, frozen melt inclusions trapped in magmatic phenocrysts, and glasses quenched from experiments at elevated pressures. Uncertainties associated with Na loss and the grow-in of Al and Si are of particular concern when EMPA is used to estimate the H_2O contents of silicate glasses (e.g., Devine et al. 1995). Optimization of the EMPA-difference method for estimating the H_2O contents of glasses becomes even more valuable in light of the recently reported systematic difference of about 25% between Fourier-trans-

0003–004X/96/0910–1176$05.00

form infrared (FTIR) spectroscopy and Karl-Fischer titration (KFT) methods [Devine et al. (1995); see Westrich (1987) for a review of KFT methodology].

From the EMPA methodologies reported in the literature, it is apparent that different combinations of beam current, spot size, and counting times are currently used to analyze hydrous glasses. To some degree, each practice is an outgrowth of transmitted knowledge and some trial and error. Although some authors acknowledge Na loss, others perhaps do not recognize it or appreciate its extent. In recent years, various corrections have been applied to Na analyses by EMPA that are quite large, often exceeding 10–15%. When coupled with the poor statistical accuracy accompanying low count rates (even at 5–10 nA incident currents) and the short counting times commonly used, such corrections lend considerable uncertainty to the compositions obtained. More important, analysts tend not to correct for Al and Si grow-in, which, because of the abundance of these elements in typical rhyolitic glasses, represents a potentially large source of error.

Standardization on glasses with compositions similar to those of the unknowns (using identical beam conditions and counting parameters) can provide good analytical results because the effects of element mobility in the standard tend to cancel those in the unknown. As this work demonstrates, however, the migratory behavior of Na depends on the H_2O content of glass, in addition to the anhydrous bulk composition. In practice, then, this method requires the acquisition of a rather large number of well-characterized glass standards (with variable H_2O contents) to be effective. Moreover, this method requires either knowledge of the approximate composition of the sample or repeated analysis with the first pass used to approximate the sample composition for the selection of appropriate standard materials. This is further complicated by the fact that the H_2O contents of alkali aluminosilicate glasses represent an unknown that is not directly measurable by EMPA, and the apparent results may be affected by analytical methods (e.g., Devine et al. 1995). The present study is directed toward answering the question "do analytical conditions exist that provide acceptable statistical accuracy while minimizing Na loss and grow-in of Al and Si in EMPA of hydrous glasses, such that little or no systematic correction to the resulting data is needed?" If such conditions can be reasonably obtained, then the analysis of hydrous glasses becomes less dependent on standard materials, and the estimation of the H_2O contents of glasses with the use of EMPA-difference methods becomes more accurate and reliable. This study is divided into two parts. This first examines changes in the X-ray intensities for Na, Al, and Si as a function of incident beam current (measured at a Faraday cup in the column) from a hydrous rhyolitic glass; those data are used to identify the conditions that optimize the analysis of hydrous glasses. The second part provides a test of these methods by the comparative analysis of a series of glasses in the albite-H_2O system from low to high H_2O content.

TABLE 1. SM35 composition

Component	wt%
SiO_2	71.77
Al_2O_3	12.72
Na_2O	4.21
K_2O	3.55
CaO	1.23
MgO	0.08
MnO	0.06
FeO*	1.25
TiO_2	0.06
F	1.07
Cl	0.16
H_2O**	4.40
O = F	−0.45
O = Cl	−0.04
Total	100.07

Note: Composition modified from Christiansen et al. (1984) to reflect total H_2O determined by ion microprobe analysis.
* Total Fe as FeO.
** Determined by ion microprobe (see text).

INTENSITY CHANGES WITH TIME IN HYDROUS RHYOLITIC GLASS

Methods

All data were obtained with a Cameca SX50 electron microprobe at the University of Oklahoma, using 15 kV accelerating potential, a static (fixed) beam, and $K\alpha$ emission from all elements. X-ray intensity vs. time data were collected on an experimentally vitrified sample of natural rhyolite (SM35) from Spor Mountain, Utah (Table 1), kindly supplied by J.D. Webster (Department of Mineral Sciences, American Museum of Natural History, New York). Experimental treatment was at 1000 °C and 2 kbar with 4.5 wt% added water. On the basis of initial H_2O content (from loss on ignition) plus H_2O added to the experimental charge, the estimated H_2O content of this material is 4.9 wt%; ion microprobe analysis of the vitrified material (using a KFT standard), however, yielded 4.4 wt% H_2O (J.D. Webster, 1995 personal communication). Optically clear fragments of the glass were embedded in epoxy within a $\frac{3}{32}$ in. brass tube, and 0.25 μm diamond grit was used for the final polish. The glass was free of cracks, contained no mineral inclusions, and appeared homogeneous within counting statistics. The Na data were collected in two analytical sessions (consecutive days) with the use of the same wavelength-dispersive spectrometer (WDS) with TAP monochromator, 1 atm counter, and identical pulse-height analysis (PHA) parameters. All Al and Si data were collected in a single analytical session, each using the same WDS configurations as Na. Spectrometers were peaked on albite from Amelia County, Virginia, by fine-scale searches with the use of 40 nA incident beam current.

X-ray intensities for Na, Al, and Si were collected at 2, 5, 10, and 20 nA beam currents. Beam diameters were 20 μm for the 2 nA beam and 15 μm for all others; beam diameters were checked qualitatively both by optical inspection of the beam on a cathodoluminescent standard (benitoite) and by secondary electron imaging and mea-

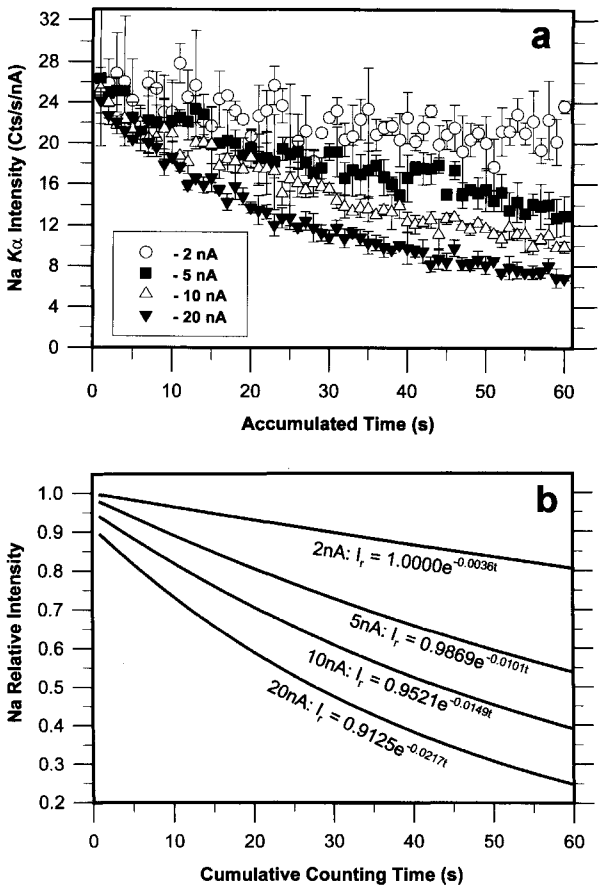

FIGURE 1. Na$K\alpha$ intensity loss in SM35 glass as a function of irradiation time. (**a**) Intensity from successive 1 s counting intervals; error bars indicate 1σ standard deviations on the basis of three to four replicate series of acquisitions. (**b**) Exponential fits of data from **a**, normalized to the zero-time intensity of the 2 nA data.

surement of contamination spots produced on andradite. No cryogenic getters were employed in the sample chamber, and the sample stage was at ambient temperature (18 °C). For each beam condition, intensities were collected using counting durations of 1, 5, 10, 20, and 40 s (additional series using 25 and 35 s durations also were acquired for Si). Counting was repeated for a cumulative continuous irradiation time of 105–120 s per spot, and a fresh sample spot was selected for intensity measurements with each counting duration (i.e., no spot was irradiated for longer than 120 s). Prior to intensity measurements, the sample was previewed by secondary electron imaging using a 1 nA beam current to ensure that no prior irradiation had occurred within 40 μm of the selected sample location. The entire procedure was repeated a minimum of three times for each counting duration at each beam condition. Although automatically regulated by the SX50, the beam current was monitored at the beginning and end of each series of intensity accumulations, and the shape and position of the beam were regularly observed on benitoite to ensure no beam drift.

Intensity changes with time

Figure 1 shows the effect of beam current on Na intensity as a function of time; for each beam current, X-ray counts for Na were summed at consecutive 1 s counting intervals with continual beam irradiation (no beam blanking). The data of Figure 1a demonstrate that Na intensity loss is most pronounced at higher beam currents, and that the loss of Na intensity is essentially immediate for beam currents >5 nA. In agreement with previous investigations on anhydrous glasses, these data suggest that the loss of Na intensity with time is best approximated by an exponential function. The data in Figure 1a were fitted to an unweighted exponential function of the form $I_t = ae^{-bt}$ (where I_t is intensity at time t, and a and b are variables fitted to the intensity data). The resultant least-squares curves, normalized to the zero-time intercept intensity from the 2 nA data, are plotted in Figure 1b. As expected, increasing beam currents result in greater exponential (b) terms, reflecting greater degrees of Na intensity loss. It is important that increasing beam currents also produced progressively lower (a) coefficient values, demonstrating that the apparent zero-time Na intensities decrease by up to about 9% from 2 to 20 nA.

The essentially immediate loss of Na observed in this study contrasts with the behavior reported for anhydrous glasses. For example, Vassamillet and Caldwell (1969) noted initial "incubation" periods of up to 25 s with no Na loss in anhydrous glasses with the use of beam currents up to 50 nA. These observations suggest that Na loss is more pronounced in hydrous than in anhydrous glasses, perhaps because of either a lower critical temperature for diffusion (e.g., Vassamillet and Caldwell 1969) or a different local chemical environment for Na (e.g., Na-O-Al in anhydrous glasses vs. association of Na with H_2O or OH in hydrous glasses: Oxtoby and Hamilton 1978; Silver and Stolper 1989; Kohn et al. 1989, 1992). The present observation that extrapolated zero-time intensities for Na decrease with increasing beam current was unexpected. Although some component of this decrease could result from the use of unweighted exponential fits (i.e., that for each curve, all data were fitted with no emphasis on the first few seconds of acquisition), it seems clear that 10 and 20 nA beams yield significantly lower intensities for the first second of analysis than do lower beam currents. Thus, for beam currents >5 nA, Na loss is apparently more rapid than can be recorded in the first second of analysis, and corrections based on extrapolation to zero-time count rates underestimate the true Na concentration.

Figures 2 and 3 show the intensity-time relations for Al and Si as a function of beam current; data were collected and treated in a manner analogous to that used for the data presented in Figure 1. For Al, both the raw data (Fig. 2a) and their unweighted exponential fits (Fig. 2b) show increased intensity at higher beam currents. As with

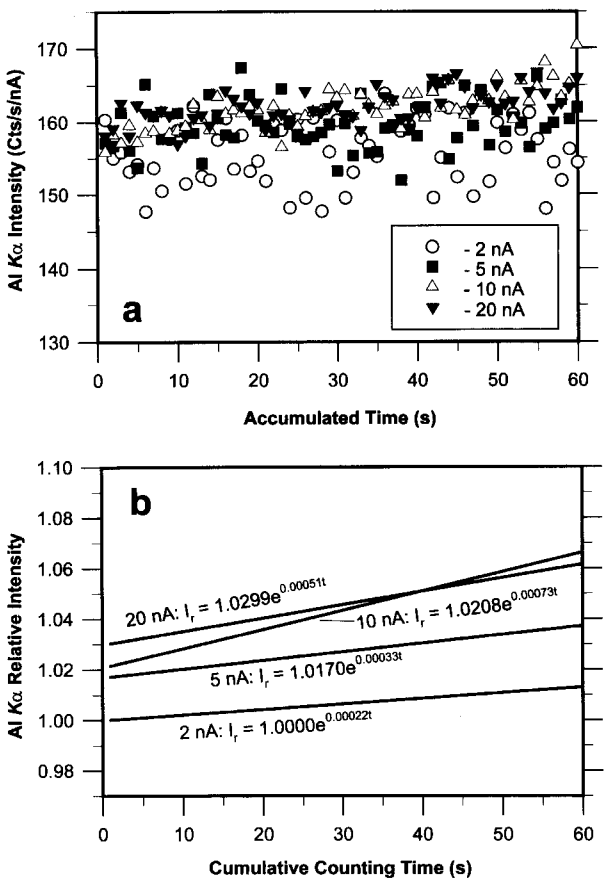

FIGURE 2. Al$K\alpha$ intensity change in SM35 glass as a function of irradiation time. (**a**) Intensity from successive 1 s counting intervals; each point represents the average of three to four replicate series of acquisitions. (**b**) Exponential fits of data from **a**, normalized to the zero-time intensity of the 2 nA data.

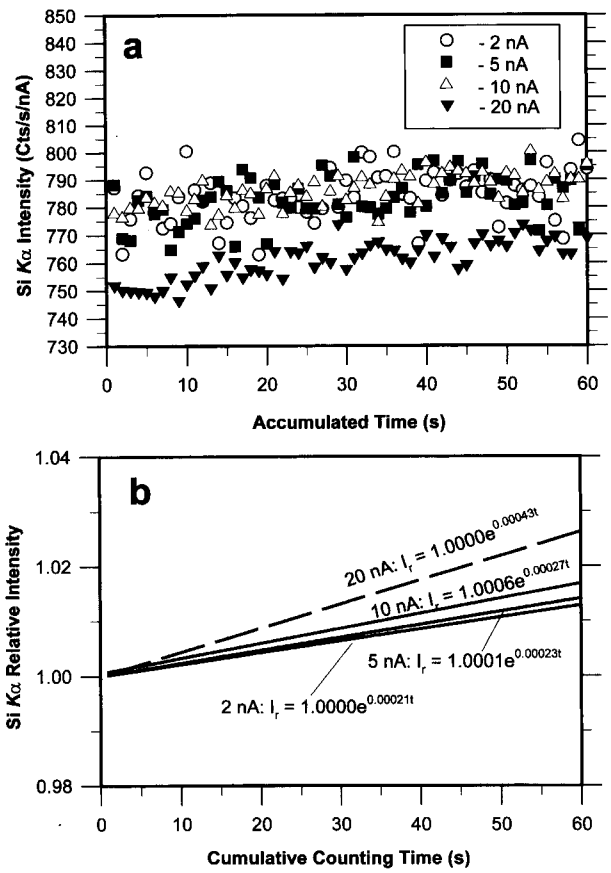

FIGURE 3. Si$K\alpha$ intensity change in SM35 glass as a function of irradiation time. (**a**) Intensity from successive 1 s counting intervals; each point represents the average of three to four replicate series of acquisitions. (**b**) Exponential fits of data from **a**; data for 2–10 nA beam currents were normalized to the zero-time intensity of the 2 nA data; data for the 20 nA beam current was normalized to the zero-time intensity of the 20 nA data.

Na, the effect is essentially immediate upon irradiation at beam currents >5 nA. The Si data (Fig. 3) show smaller changes in relative intensity with time, and smaller differences in that change as a function of beam current, in comparison with Na and Al. Note in Figure 3a that the 20 nA beam yielded lower intensities, in terms of counts per second per nanoampere, than did the lower beam currents; this probably resulted from high count rates (>15000 cps) that exceeded the linear range of detector response for the combination of bias and dead-time correction employed. The exponential fit for the 20 nA data in Figure 3b (dashed curve) was normalized to the zero-time intercept interpolated from the 20 nA data, rather than the 2 nA data; therefore, the relation between this curve and those from lower beam currents is somewhat more uncertain than for Na and Al (especially at zero-time).

As noted above, the grow-in behaviors of Al and Si are somewhat different. The increase in relative intensity with increasing beam current is greater for Al than for Si. For all but the 2 nA beam current, Al also demonstrates a greater increase in intensity with prolonged irradiation. These effects probably result from the fact that Na absorbs the $K\alpha$ X-rays of Al more strongly than it does those of Si (i.e., the mass absorption coefficient of Na for Al$K\alpha$ is about 1.55 times that for Si$K\alpha$: see Heinrich 1966). Therefore, the diffusional loss of Na from the excitation volume results in an increase in the Al/Si ratio of emitted X-rays.

Time-integrated vs. instantaneous intensities

The intensities discussed up to this point represent essentially instantaneous values (counts per second per nanoampere), as a function of irradiation time. Intensities measured during microprobe analysis are not instantaneous values but represent a time integration (average) of the instantaneous values over the course of the counting interval. With this in mind, an examination of time-integrated intensities may be more instructive for selecting analytical conditions that optimize the analysis of glasses.

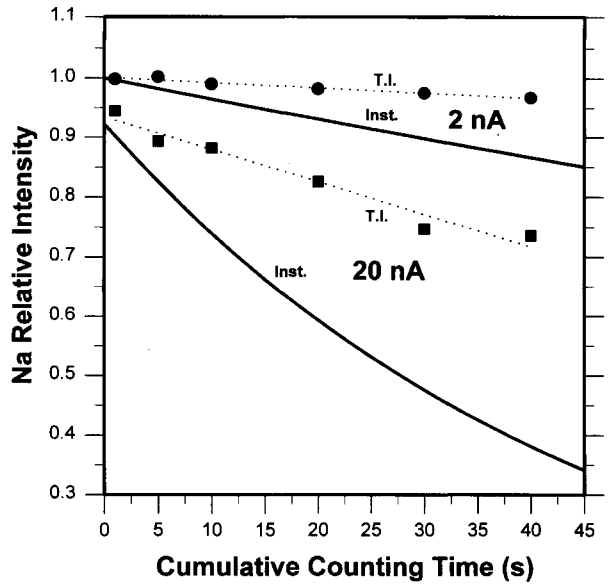

FIGURE 4. Time-integrated (T.I.) vs. instantaneous (Inst.) relative intensities for Na$K\alpha$ X-rays in SM35 glass for 2 nA (circles) and 20 nA (squares) beam conditions.

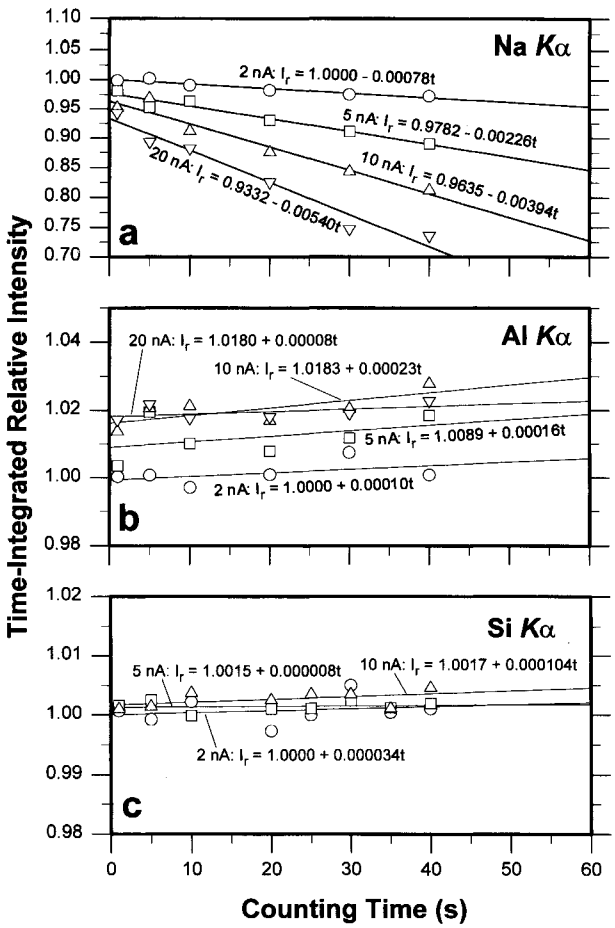

FIGURE 5. Time-integrated relative intensities as a function of counting time for (a) Na$K\alpha$, (b) Al$K\alpha$, and (c) Si$K\alpha$ X-rays in SM35 glass. Relative intensities were derived by normalization of raw data to the zero-time count rates for each component at 2 nA; all points represent the averages of four to six acquisitions at each counting interval. Circles = 2 nA, squares = 5 nA, triangles = 10 nA, inverted triangles = 20 nA.

For mobile components like Na, it would be expected that the time-integrated intensities at extended counting intervals are greater than those of the instantaneous (1 s) count rate at the termination of analysis; an opposite relation would be anticipated for components such as Al and Si, the intensities of which grow-in with time. This is shown schematically for Na in Figure 4, which compares the (time-averaged) relative intensities for counting durations up to 40 s with the exponential fits of the instantaneous values at 2 and 20 nA. Note that although instantaneous intensity-time relations are best approximated by an exponential function, changes in time-integrated intensities are apparently well described by a linear function of time.

Figure 5 shows the time-integrated relative intensities for Na, Al, and Si normalized to their zero-time count rates derived from the exponential fits to acquisitions at 2 nA. As was seen for the instantaneous intensities, the time-integrated relative intensities for Na and Al display, respectively, lower and higher zero-time intercept values for beam currents ≥ 5 nA; there is little significant change for Si at beam currents ≤ 10 nA. More importantly, the slopes for the time-integrated curves are quite small at low beam current (2 nA) but generally increase with increasing beam current.

Minimizing analytical uncertainty

Excluding the effects of changing count rates during the irradiation of a sample, the most important factor in assessing analytical uncertainty is the total number of accumulated counts above mean background. For a given counting duration, analytical uncertainty (defined as $N^{1/2}/N$, where N = number of counts) is greater at lower beam currents. The same analytical uncertainty can be achieved using either high beam currents at short counting times or low beam currents at longer counting times as illustrated for Na in the SM35 composition in Figure 6. For components in glass that show changes in intensity as a function of irradiation time, the combined effects of accumulated counts and intensity change during prolonged beam exposure must be considered. Figures 5a and 6 clearly show that for Na, the most problematic of the alkali aluminosilicate components in glass, X-ray intensity loss and analytical uncertainty are minimized by using low beam current (2 nA) and long counting times (20–40 s). This is consistent with the suggestion of Spray and Rae (1995) that incident beam currents of <100 mW (corresponding to about 6.7 nA at 15 kV, or 5 nA at 20 kV) should be used for analyzing Na-bearing silicate

glasses. Of equal importance to incident beam current, however, is the current density at the sample. Test analyses on the SM35 glass using a 2 nA incident beam current and 5 μm spot size (not reported) show a 15–21% loss of Na intensity after 30–40 s of irradiation. When compared with the minimal loss using a 20 μm spot size, reported above, this indicates that the beam diameter should be as large as practical while retaining proper X-ray focus at the edge of the excitation volume (i.e., 15–20 μm). Using these methods we found that the loss of Na intensity is comparable to, or less than the analytical uncertainty (based on counting statistics), such that correction of the data is typically not warranted. This removes the necessity of large corrections for Na on the basis of extrapolated zero-time count rates required by the use of higher beam currents (which themselves carry significant uncertainties associated with derivation by successive short counting intervals; see Fig. 6) and the noted decrease in zero-time count rates at higher beam currents. Some proponents of energy-dispersive (EDS) methods (e.g., Goodhew and Gulley 1974; Spray and Rae 1995) have suggested that long counting times are counterproductive for glass analysis at the beam currents required by WDS analysis (purportedly $\geq$5 nA). This suggestion is contrary not only to the current findings but also to the observation of Spray and Rae (1995) that no Na was lost in four repeated analyses of the same spot in basaltic glass with the use of a 2.5 nA beam with 20 μm defocused spot. Moreover, EDS methods are not practical in many cases because many combinations of microprobe hardware and automation software do not support integrated WDS-EDS analysis; therefore, optimized WDS-based methods of analysis are needed. With the conditions described above for the SM35 composition, counting times of 20–40 s yield calculated minimum detection levels (at 3σ above mean background) of 0.07–0.05 wt% Na_2O with analytical uncertainties of 2–3% (relative), and a maximum loss of Na intensity of 2–3% (relative) by WDS.

From Figures 5b and 5c it can also be seen that the use of a 2 nA, 20 μm beam and long counting times effectively eliminates the grow-in of Si and Al. Therefore, these beam conditions minimize the analytical uncertainties for these components both in terms of the magnitude of accumulated counts and in the mathematical correction for this phenomenon. This latter point is especially problematic and difficult to quantify, considering the different grow-in behaviors exhibited by Al and Si and the statistical uncertainties for determining their zero-time count rates by extrapolation from successive short counting intervals (e.g., 1–2 s). Moreover, it must be considered that glass dehydration during analysis would elevate the concentrations of other components in the excitation volume, thus leading to artificially high contents of immobile components and low H_2O contents by difference of EMPA totals from 100%. Although this is not rigidly testable with the data presented so far, simple mass balance based on intensity data and the SM35 composition suggests that apparent increases in Al_2O_3 and SiO_2 contents (in weight percent), monitored by their intensity changes, are greater than the loss of Na_2O for beam currents $\geq$5 nA.

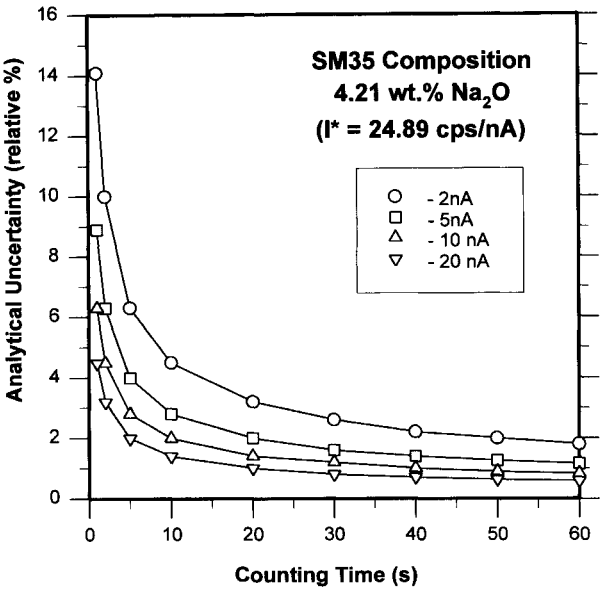

FIGURE 6. Analytical uncertainty [$\equiv 100(N^{1/2}/N)$, where N = total counts above mean background] for Na in SM35 glass as a function of counting time. Intensities for calculations are based on the zero-time count rate for Na$K\alpha$ at 2 nA ($\equiv$I*), which was derived by exponential fit to the raw data in Figure 1a.

TESTING BY APPLICATION: ANALYSIS OF Ab-H_2O GLASSES

Methods

Analyses were performed on a series of albite-H_2O glasses, graciously provided by Sally Newman and Edward Stolper of the California Institute of Technology. The glasses correspond to sample numbers A1009, ABC-11, LAS-22, and LAS-21 reported in Silver and Stolper (1989), which FTIR analyses showed to contain 2.2 (AB2W), 4.94 (AB5W), 6.99 (AB7W), and 9.65 (AB10W) wt% H_2O (note that 4.93 wt% water in sample ABC-11 was also verified by H_2 manometry). All EMP analyses used 15 kV accelerating potential and feldspar standards. All elements were analyzed simultaneously, and data reduction employed the PAP procedure (Pouchou and Pichoir 1985). Analyses were replicated using (1) a 2 nA beam with 20 μm diameter, and counting times of 30 s for all elements (analytical uncertainties for Na $\leq$2% relative); (2) a 10 nA, 15 μm beam, and counting times of 5 s for all elements; and (3) a 20 nA, 15 μm beam, and counting times of 5 s for all elements. On the basis of counting statistics, conditions 1 and 2 provide comparable analytical uncertainties ($\leq$2% relative for Na), whereas condition 3 should provide slightly smaller uncertainties because of higher count rates. Minimum levels

TABLE 2. Uncorrected and corrected EMPA of albite-H_2O glasses

	2 nA, 30 s			10 nA, 5 s			20 nA, 5 s			
	EMPA*	SI**	SI + Int†	EMPA	SI	SI + Int	EMPA	SI	SI + Int	Calc.‡
AB2W		$n = 20$			$n = 18$			$n = 17$		
SiO_2	66.37	66.30	66.30	66.65	66.62	66.50	66.91	66.84	66.61	66.56
Al_2O_3	19.67	19.61	19.61	19.84	19.82	19.46	19.91	19.90	19.54	19.57
Na_2O	11.03	11.28	11.28	10.91	11.13	11.56	10.83	11.13	11.95	11.24
K_2O	0.21	0.21	0.21	0.24	0.24	0.24	0.21	0.21	0.21	0.15
CaO	0.26	0.26	0.26	0.24	0.24	0.24	0.27	0.27	0.27	0.25
Total	97.54	97.66	97.66	97.88	98.05	98.00	98.13	98.35	98.58	97.77
H_2O(D)§	2.46	2.34	2.34	2.12	1.95	2.00	1.87	1.65	1.42	2.22
AB5W		$n = 24$			$n = 12$			$n = 16$		
SiO_2	64.49	64.42	64.42	64.77	64.74	64.63	64.81	64.74	64.58	64.72
Al_2O_3	19.03	18.97	18.97	19.49	19.39	19.02	19.10	19.09	18.75	19.02
Na_2O	10.67	10.93	10.93	10.50	10.71	11.13	10.15	10.43	11.09	10.93
K_2O	0.17	0.17	0.17	0.18	0.18	0.18	0.17	0.17	0.17	0.14
CaO	0.16	0.16	0.16	0.19	0.19	0.19	0.18	0.18	0.18	0.25
Total	94.52	94.65	94.65	95.13	95.21	95.15	94.41	94.61	94.77	95.06
H_2O(D)	5.48	5.35	5.35	4.87	4.79	4.85	5.59	5.39	5.23	4.94
AB7W		$n = 43$			$n = 8$			$n = 10$		
SiO_2	62.97	62.90	62.90	63.19	63.16	63.08	63.42	63.35	63.19	63.32
Al_2O_3	18.44	18.38	18.38	18.75	18.73	18.39	18.70	18.69	18.36	18.62
Na_2O	10.18	10.43	10.43	9.80	10.01	10.39	9.41	9.68	10.38	10.69
K_2O	0.21	0.21	0.21	0.21	0.21	0.21	0.21	0.21	0.21	0.14
CaO	0.24	0.24	0.24	0.25	0.25	0.25	0.25	0.25	0.25	0.24
Total	92.04	92.16	92.16	92.20	92.36	92.32	91.99	92.18	92.39	93.01
H_2O(D)	7.96	7.84	7.84	7.80	7.64	7.68	8.01	7.82	7.61	6.99
AB10W		$n = 22$			$n = 12$			$n = 15$		
SiO_2	61.54	61.47	61.47	62.19	62.16	62.05	62.31	62.25	62.09	61.51
Al_2O_3	18.21	18.15	18.15	18.38	18.35	18.03	18.43	18.42	18.10	18.08
Na_2O	10.01	10.26	10.26	9.46	9.65	10.02	9.03	9.28	9.96	10.38
K_2O	0.21	0.21	0.21	0.20	0.20	0.20	0.22	0.22	0.22	0.14
CaO	0.23	0.23	0.23	0.25	0.25	0.25	0.25	0.25	0.25	0.23
Total	90.20	90.32	90.32	90.48	90.61	90.55	90.24	90.42	90.62	90.34
H_2O(D)	9.80	9.68	9.68	9.52	9.39	9.45	9.76	9.58	9.38	9.65

Note: All analyses performed using 15 kV accelerating potential; beam currents and counting times are specified.
* Uncorrected values from EMPA.
** EMPA results corrected for slope of integrated intensity vs. time shown in Figure 5.
† EMPA results corrected for slope and zero-time intercept shown in Figure 5.
‡ Calculation based on amelia albite composition and H_2O from FTIR calibration of Silver and Stolper 1989.
§ H_2O determined by difference of EMPA total from 100%.

of detection for all oxide components were between 0.06 and 0.09 wt% on the basis of statistics from analysis of the standards.

Results and discussion

The comparisons of EMPA results with glass compositions calculated for Amelia albite plus H_2O (determined by FTIR) are shown in Table 2. Included in this table are the uncorrected results (EMPA) and corrections based on only the slope (Sl) and the slope plus decreased zero-time intensity values (Sl + Int) deduced from the time-integrated intensity changes for Na, Al, and Si shown in Figure 5. The results of analyses using the 2 nA beam current are in excellent agreement with the calculated values for all elements, and corrections to the raw data are small (relative percents: Na 2.4, Al 0.3, Si 0.1). With the exception of sample AB7W (LAS-22), H_2O contents derived from difference of EMPA from 100% agree with the FTIR results of Silver and Stolper (1989) to within 0.41 wt%, with an average difference of 0.19 wt%. For sample LAS-22, H_2O contents derived by difference (for all beam conditions) are systematically higher than FTIR values by 0.62–1.02 wt%; because the other samples (with both higher and lower H_2O contents) show more reasonable agreement, our only explanations for this observation are heterogeneity within the glass (observed by analysis) and a potential error in the original FTIR determination (we note that about 8 wt% H_2O was added to that charge prior to synthesis at 15 kbar; Silver and Stolper, 1987 personal communication).

As expected from the previous studies of intensities, the uncorrected data from analyses using 10 and 20 nA beam currents show demonstrably lower Na_2O and somewhat higher Al_2O_3 and SiO_2 contents in comparison with the calculated compositions of the glasses. For the most part, correction of the raw data on the basis of only the slope of time-integrated intensity variations also demonstrates lower Na_2O and higher Al_2O_3 and SiO_2 contents than the calculated compositions. With some exceptions (discussed below), correction of the raw data on the basis of both the slope and the decrease in zero-time intensity with increased beam current produces better agreement. This latter observation demonstrates the importance of (primarily Na and Al) intensity changes during the first second of analysis; at higher beam currents, changes in the observed zero-time intensities in

hydrous glasses can lead to systematic analytical errors when simple intensity vs. time corrections are used. It must be considered that the apparent absence of a zero-time intensity decrease for the data acquired at 2 nA is artificial; i.e., that relative to even lower beam currents, the use of a 2 nA beam would demonstrate changes in zero-time intensities just as the higher beam currents do relative to the data acquired at 2 nA. Although this is probably true, two lines of evidence suggest that such changes are small in comparison with the relative changes seen at higher beam currents: (1) Changes are comparatively small on increasing current from 2 to 5 nA (e.g., Figs. 1–3 and 5), indicating a proportionate decrease in the magnitude of change at lower beam currents; and (2) true zero-time intensities significantly different from those observed at 2 nA should lead to systematic differences in the analyzed vs. calculated compositions of the glasses (e.g., a higher true zero-time intensity for Na would result in low Na_2O values, and vice versa for Al_2O_3 and SiO_2), which is not observed.

In Table 2, some discrepancies between calculated compositions and slope + intercept–corrected analytical results are obvious for 10 and 20 nA beams. For the AB2W glass, corrected Na_2O results are high (especially for the 20 nA beam), whereas corrected Na_2O results are low for the AB7W and AB10W glasses. This observation is probably related to the variable mobility of Na as a function of H_2O content. The corrections applied to these analyses were derived from the intensity studies of the SM35 glass containing about 4.4–4.9 wt% H_2O. It appears, therefore, that these factors overcorrected Na_2O in the glasses with low H_2O contents because of lower rates of Na migration; conversely, these factors undercorrected for Na_2O in glasses with higher H_2O contents, in which Na mobility is enhanced. By this reasoning, we would expect the corrected analytical results at 10 and 20 nA for the AB5W glass to be in excellent agreement with the calculated values; such agreement is observed.

The method of analysis described in this section utilized anhydrous crystalline standard materials to analyze hydrous glasses. From the discussion above, it should be clear that the use of a 2 nA, 20 μm beam and counting times of 30 s provided excellent results, with only small corrections to the original EMPA data and counting statistical uncertainties comparable to (or slightly better than) those obtained at higher beam currents. It should be emphasized, however, that the use of anhydrous standards coupled with corrections to intensities on the basis of the analysis of a secondary hydrous standard glass can lead to significant errors for incident beam currents $\geq$5 nA. These errors would result primarily because the changes of zero-time intensities from true values observed for components in hydrous glasses would not be recognizable. The corrections obtained from such secondary standards would therefore yield values akin to the slope (-only) corrections in Table 2, which yield low values for Na and high values for Al and Si. Even if the true zero-time intensity could be deduced (e.g., the slope + intercept correction in Table 2), the above results indicate that errors will still be introduced unless the H_2O content of the secondary standard glass is comparable to that of the unknown. Finally, from Table 2 it can be seen that the degree of Na migration is affected by the H_2O content of glass; for the 20 nA beam, $Na_2O_{EMPA}/Na_2O_{Calc}$ decreases from 0.96 to 0.87 as H_2O increases from 2.22 to 9.65 wt%. Therefore, analytical methods utilizing glasses as primary standards and incident beam currents $\geq$5 nA also should utilize standard glasses with H_2O contents similar to the samples to be analyzed.

Elevated backscattered electron-signal intensities for EMPA spots provide evidence of glass densification resulting from dehydration, Na migration, or both. The ultimate fate of the hydrous component of glass during analysis is uncertain. One might intuit that dehydration should be at least as rapid as the rate of Na migration, leading to elevated concentrations of other components in the excitation volume. In this case, we would expect the H_2O determined by EMPA-difference methods to be lower than the calibrated values and to be systematically and increasingly underestimated with increasing incident beam current. This does not appear to be borne out by the present analyses, although small decreases in H_2O by difference were observed in both the uncorrected and corrected results for Ab-H_2O glasses (Table 2). Note that although corrections to the original EMPA data resulted in changes among the relative proportions of Na_2O, Al_2O_3, and SiO_2, corrections had little effect on the derivation of H_2O by difference. We caution, however, that this relation holds only when corrections are applied to Na, Al, and Si; correction of only Na results in a systematic underestimation of H_2O by difference. As can be deduced from Table 2, the use of corrected values for only Na_2O with the original EMPA data in this study results in the underestimation of H_2O by an average of 0.61 wt% at 10 nA and 0.99 wt% at 20 nA for glasses of all H_2O contents (representing 25–50% errors for glasses with lower H_2O contents).

Recommendations for hydrous glass analysis

Analytical conditions

For the analysis of Na, K, Al, and Si, we recommend the use of a 2 nA incident beam current, 20 μm spot, and counting times of 20–40 s. Rastered beam modes are unnecessary, and beam diameters >20 μm should be avoided because X-rays generated much farther than about 10 μm from the axial center of the beam are out of focus for (vertical) WD spectrometers for most microprobes. We recognize that there are many cases (e.g., the analysis of melt inclusions or experimental crystal-melt systems) in which the use of a 20 μm spot is not possible. The analyst is cautioned that decreasing the spot size of even a 2 nA beam results in increased migration of Na in hydrous glasses, and thus correction of the results must be addressed.

Na and Al should be analyzed first and simultaneously.

If the selection of monochromators permits, Si and K should be analyzed simultaneously with Na and Al. If configuration does not permit this, Si should be analyzed afterward because its intensity grow-in with time is less significant than that of Al. This suggestion is supported by our test results showing no increase in the uncorrected SiO_2 values when Si is analyzed after Al on the same spectrometer (with the recommended 2 nA beam current), in comparison with the simultaneous analysis of Na, Al, and Si. For other (minor, trace, and light element) components, we recommend the use of a second beam condition such as 20 nA incident current and 20 μm spot beam. This permits higher count rates, and the effects of Na migration on the relative accuracies of most minor to trace level components should be negligible (note that intensity changes with time as a function of beam current for components such as F, P, and B are yet to be determined). Most modern microprobe-automation software packages support multicondition analyses. Although somewhat more time consuming than a single condition at high beam currents, automated analysis with two (or more) conditions requires little more effort.

Correction procedures

To reproduce accurately the major alkali aluminosilicate compositions of the analyzed glasses, corrections should be applied to Na, Al, and Si. As described above, correction of only Na leads to a systematic underestimation of H_2O by difference of EMPA totals from 100% and inaccurate (underestimated) Na/Al and ASI [aluminum saturation index, defined as the molecular ratio $Al_2O_3/(Na_2O + K_2O + CaO)$]. These errors are especially important if beam currents higher than 2 nA are used. Although preliminary study suggests that the migration of K is not significant with a 2 nA and 20 μm beam, correction for K loss also should be considered if higher beam currents or smaller spot sizes are to be used. Ideally, intensity corrections should be applied prior to data reduction (i.e., PAP or ZAF calculations), but tests with analyses in this study showed no significant differences when corrections derived from time-integrated intensity changes were simply applied to the weight-percent values obtained from EMPA.

The use of time-integrated intensities, as presented in Figure 5, represents a simpler and more direct method of correcting data than does extrapolation of instantaneous intensities to zero-time values. It is simpler because intensity changes as a function of cumulative counting time closely approximate a linear function rather than the exponential function described by instantaneous intensities. It is more direct because microprobe analysis does not simply measure the instantaneous intensities but rather records their time average over the course of the analysis interval. Correcting the time-averaged intensities from EMPA to apparent zero-time values can lead to systematic errors in correction for counting intervals of more than a couple seconds. For example, Figure 4 shows that the time-integrated intensity for Na is greater than the instantaneous intensity at the end of analysis; correction of the averaged intensity at the end of analysis to the zero-time value would thus overestimate the true Na count rate. The opposite would hold for Al and Si, for which extrapolation to zero-time would underestimate true count rates. Of course these corrections hold only insofar as the true zero-time intensities can be measured. As demonstrated previously, rapid Na migration in hydrous glasses causes the apparent zero-time intensities to decrease with increasing beam currents above 5 nA. Using 10 and 20 nA beam currents in this study, we were successful in obtaining reasonable Na_2O values for albitic glasses with $\geq$5 wt% H_2O only by correcting for the effects of depressed zero-time intensities relative to values acquired at 2 nA (e.g., compare the Sl- vs. Sl + Int–corrected Na_2O values for 10 and 20 nA conditions).

Measuring H_2O in glass by difference

With care in electron microprobe analysis, errors stemming from Na loss and Al and Si grow-in can be corrected or, by the use of a low-energy defocused beam, nearly eliminated altogether. In this study, we used anhydrous standards to analyze experimental glasses with H_2O contents up to nearly 10 wt% H_2O as determined by FTIR, and our calculations of H_2O by difference of EMPA totals from 100 wt% yield excellent agreement with the FTIR values. We conclude that the EMPA methods presented here make estimation of H_2O in glass by difference a viable and accurate procedure for glasses containing $> \sim 1$ wt% H_2O, which agrees with the findings of Devine et al. (1995). We do not suggest, however, that EMPA difference methods can completely supplant other methods of H_2O determination such as FTIR, ion microprobe (SIMS), or KFT for bulk samples. These latter methods provide for the direct determination of H_2O and are more sensitive for glasses with low H_2O contents; as such, they are excellent for assessing the results from EMPA difference, especially where small spot sizes and high beam currents introduce large error in the EMPA. We note, however, that each method carries its own uncertainties. For FTIR analysis, these primarily hinge on the compositional sensitivity of extinction coefficients. Analysis by SIMS can only be as accurate as the (glass) standard materials used for calibration, for which H_2O contents are typically determined either by FTIR or Karl-Fischer titration. Devine et al. (1995) noted large systematic differences of H_2O in glass by FTIR vs. KFT. The agreements between H_2O determination by FTIR and EMPA difference in Devine et al. (1995) and the current study suggest erroneously low yields by KFT, at least for H_2O-rich glasses.

Acknowledgments

The Electron Microprobe Laboratory at the University of Oklahoma was established by grant DE-FG22-87FE1146 from the U.S. Department of Energy. Recent upgrades to computer automation and imaging hardware were made with support from NSF grant EAR-9404658. The authors thank the University of Oklahoma Office of Research Administration for their continuing support of the microprobe laboratory. We also thank Ian Steele, Malcolm Rutherford, and David Mogk, whose editorial reviews enhanced the quality of this manuscript.

REFERENCES CITED

Borom, M.P., and Hanneman, R.E. (1967) Local compositional changes in alkali silicate glasses during electron microprobe analysis. Journal of Applied Physics, 38, 2406–2408.

Christiansen, E.H., Bikun, J.V., Sheridan, M.F., and Burt, D.M. (1984) Geochemical evolution of topaz rhyolites from the Thomas Range and Spor Mountain, Utah. American Mineralogist, 69, 223–236.

Devine, J.D., Gardner, J.E., Brack, H.P., Layne, G.D., and Rutherford, M.J. (1995) Comparison of microanalytical methods for estimating H_2O contents of silicic volcanic glasses. American Mineralogist, 80, 319–328.

Goodhew, P.J. (1975) Electron probe microanalysis of glass containing alkali metals. Microstructural Science, 3, 631–641.

Goodhew, P.J., and Gulley, J.E.C. (1974) The determination of alkali metals in glasses by electron probe microanalysis. Glass Technology, 15, 123–126.

Heinrich, K.F.J. (1966) X-ray absorption uncertainty. In T.D. McKinley, K.F.J. Heinrich, and D.B. Wittry, Eds., The electron microprobe, p. 296–377. Wiley, New York.

Kohn, S.C., Dupree, R., and Smith, M.E. (1989) A multinuclear magnetic resonance study of the structure of hydrous albite glasses. Geochimica et Cosmochimica Acta, 53, 2925–2935.

Kohn, S.C., Dupree, R., and Mortuza, M.G. (1992) The interaction between water and aluminosilicate magmas. Chemical Geology, 96, 399–409.

Kushiro, I. (1972) Effect of water on the composition of magmas formed at high pressures. Journal of Petrology, 17, 139–193.

Lineweaver, J.L. (1962) Oxygen outgassing caused by the electron bombardment of glass. Journal of Applied Physics, 34, 1786–1791.

Nielsen, C.H., and Sigurdsson, H. (1981) Quantitative methods for electron microprobe analysis of sodium in natural and synthetic glasses. American Mineralogist, 66, 547–552.

Oxtoby, S., and Hamilton, D.L. (1978) The discrete association of water with Na_2O and SiO_2 in NaAl silicate melts. Contributions to Mineralogy and Petrology, 66, 185–188.

Pouchou, J.L., and Pichoir, F. (1985) "PAP" (ϕ-ρ-Z) correction procedure for improved quantitative microanalysis. In J.T. Armstrong, Ed., Microbeam analysis, p. 104–106. San Francisco Press, California.

Silver, L., and Stolper, E. (1989) Water in albitic glasses. Journal of Petrology, 30, 667–709.

Spray, J.G., and Rae, D.A. (1995) Quantitative electron-microprobe analysis of alkali silicate glasses: A review and user guide. Canadian Mineralogist, 33, 323–332.

Varshneya, A.K., Cooper, A.R., and Cable, M. (1966) Changes in composition during electron microprobe analysis of K_2O-SrO-SiO_2 glass. Journal of Applied Physics, 37, 2199–2202.

Vassamillet, L.F., and Caldwell, V.E. (1969) Electron-probe microanalysis of alkali metals in glasses. Journal of Applied Physics, 40, 1637–1640.

Watkins, N.D., Sparks, R.S.J., Sigurdsson, H., Huang, T.C., Federman, A., Carey, S., and Ninkovich, D. (1978) Volume and extent of the Minoan tephra from Santorini volcano: New evidence from deep-sea sediment cores. Nature, 271, 122–126.

Westrich, H.R. (1987) Determination of water in volcanic glasses by Karl-Fischer titration. Chemical Geology, 63, 335–340.

MANUSCRIPT RECEIVED SEPTEMBER 25, 1995
MANUSCRIPT ACCEPTED JUNE 5, 1996